Journal of Inorganic and General Chemistry
ZAAC
Zeitschrift für anorganische und allgemeine Chemie
DOI: 10.1002/zaac.202000228
ARTICLE

On New Staudinger Type Reactions of Phosphorus Centered Biradicaloids, $[P(\mu\text{-}NR)]_2$ (R = Ter, Hyp), with Ionic and Covalent Azides

Axel Schulz,*[a,b] Alexander Hinz,[a] Anne Rölke,[a] Alexander Villinger,[a] and Ronald Wustrack[a]

Dedicated to Professor Dr. Thomas M. Klapötke on the Occasion of his 60th Birthday

Abstract. Phosphorus centered biradicaloids of the type $[P(\mu\text{-}NTer)]_2$ [R = Ter = terphenyl = 2,6-bis(2,4,6-trimethylphenyl)phenyl, Hyp = tris(trimethylsilyl)silyl] were treated with covalent ($R\text{-}N_3$) and ionic azides (AgN_3 and $Hg(N_3)_2$). While the reaction with the ionic azides led exclusively to the formation of diazides, $[N_3P(\mu\text{-}NTer)]_2$, triaza-diphospha-pentadienes, RN=P–N(R′)–P=NR, were observed in the reaction with covalent azides featuring a Staudinger type reaction followed by PN bond rearrangement reactions. This new Staudinger type mechanism as well as the structure, bonding and thermodynamics along different reaction paths are discussed based on DFT computations.

Introduction

As early as 1864, *Griess* was able to isolate the first organic azide, phenylazide.[1,2] In 1890 *Curtius* succeeded in preparing the parent compound HN_3, hydrazoic azide (hydrogen azide), and some metal azide salts,[3] which can generally be regarded as the birth of inorganic, covalent azide chemistry.[4–7]

With respect to small molecule activation, progress in main group chemistry in the last decade was mainly achieved by applying new concepts like frustrated Lewis pairs (FLPs),[8–11] low-valent species with open coordination sites,[12] N-heterocyclic carbenes,[13–20] persistent radicals,[21] and biradicaloids,[22–24] or main group compounds with multiple bonds.[25] Most of these concepts take advantage of bulky substituents to stabilize unusual bond situations.[25] It was *P. P. Power*, who recognized that under specific conditions the heavier main group elements can be considered transition metal mimics.[26]

Especially, four-membered heterocycles,[27–43] containing either open shell singlet or triplet biradical character, have been in the focus over the last three decades. Due to their unusual bond situation with two unpaired electrons (Scheme 1, e.g. Lewis formula **I**), which interact transannularly,[23,24] these species feature a special reactivity and can be used to activate bonds in small molecules. Moreover, a closer look at the electronic situation as depicted in Scheme 1 reveals that also ionic bonding (zwitterion formation, **II** – **V**)[44,45] plays an essential role in the resonance Scheme and might even be considered as a transannular FLP situation contributing to the often observed remarkable reactivity. In terms of MO theory, this reactivity can be attributed to the transannularly antibonding HOMO of the biradicaloid, which can interact with the empty σ* or π* LUMOs of the substrate molecule (Scheme 2). Since the HOMO–LUMO gap of biradicaloids is usually rather small, the LUMO is occupied to a significant extent leading to a biradical character commonly ranging between 20–30% for

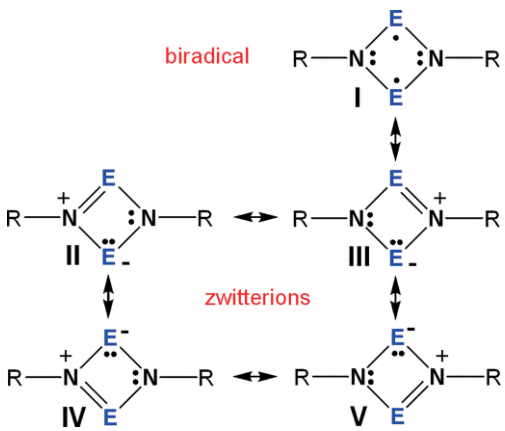

Scheme 1. Valence bond description of four-membered biradicaloids of the type $[E(\mu\text{-}NTer)]_2$ (E = P – Bi).

* Prof. Dr. A. Schulz
E-Mail: axel.schulz@uni-rostock.de
[a] Anorganische Chemie, Institut für Chemie
Universität Rostock
Albert-Einstein-Str. 3a
18059 Rostock Germany
[b] Material Design
Leibniz-Institut für Katalyse an der Universität Rostock
Albert-Einstein-Str. 29a
18059 Rostock Germany
Supporting information for this article is available on the WWW under **http://dx.doi.org/10.1002/zaac.202000228** or from the author.

four-membered heterocyclic biradicaloids, which, however, can increase the heavier the atoms involved.[46,47]

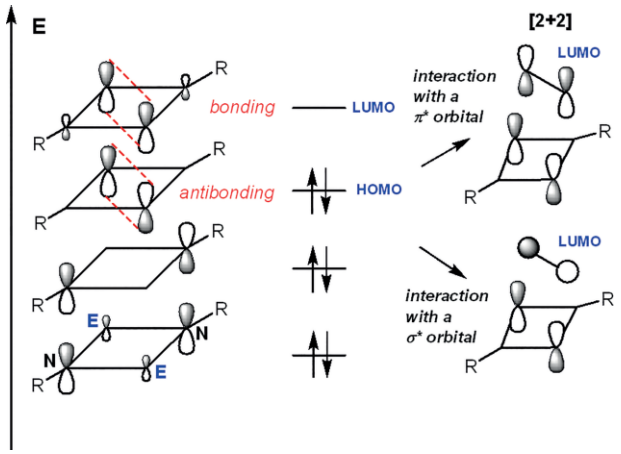

Scheme 2. Left: MO description of four-membered biradicaloids of the type $[E(\mu\text{-NTer})]_2$ (E = P – Bi). Right: $HOMO_{biradicaloid}$-LUMO [2+2] interaction of $[E(\mu\text{-NTer})]_2$ with molecules containing π- or σ-bonds.

Recently, we have shown that pnictogen centered biradicaloids of the type $[E(\mu\text{-NR})]_2$ (E = P, As, Sb, Bi; R = Ter, Hyp) can be generated and utilized for the activation of molecules bearing single, double and triple bonds.[48–51] While $[E(\mu\text{-NR})]_2$ with E = P and As can be prepared in bulk,[51–54] the heavier congeners are only of fleeting existence in solution,[47] but once prepared in situ, they can also be used for the activation of small molecules. For example, $[E(\mu\text{-NR})]_2$ (E = P, As, Sb, Bi; R = Ter) reacts readily with alkenes or alkynes forming [2.1.1]bicyclic structures (Scheme 3, product **A**).[47,50,51,55–57] Interestingly, with a small substituent at the alkyne such as R = H, the addition product **B** rearranges slowly upon thermal treatment to afford a [3.1.0]bicycle **C**,[58] which is not the observed for bulky substituents (e.g. R = Ph).

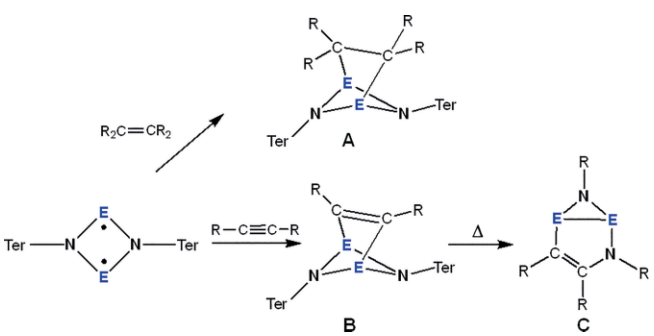

Scheme 3. [2+2] reaction of $[E(\mu\text{-NR})]_2$ with alkenes and alkynes forming [2.1.1]bicyclic structures (**A** and **B**). Addition product **B** can thermally rearrange affording [3.1.0]bicycle **C**.

To the best of our knowledge, the reaction of ionic and covalent azides, species with a multiple nitrogen–nitrogen multiple bond, and biradicaloids has not been studied yet. Here we want to report on the reactivity of different azides towards phosphorus centered four-membered biradicaloids $[P(\mu\text{-NR})]_2$ (R = Ter, Hyp).

Results and Discussion

Addition of Ionic Azides

In a first series of experiments, we studied the reaction of $[P(\mu\text{-NTer})]_2$ (**1**Ter) with AgN_3 and $Hg(N_3)_2$. The idea was to oxidize the phosphorus atom by Ag^+/Hg^{2+} ions and to transfer the azide ion to the P^+ center thereby forming a polar P–N_3 bond (Scheme 4). Indeed, this concept nicely worked and $[N_3P(\mu\text{-NTer})]_2$ (**2**Ter) was obtained in good yields [51 % AgN_3, 77 % $Hg(N_3)_2$, Figure 1]. No Staudinger type reaction was observed because the phosphorus atom is too electron-deficient. It should be noted that the reaction with AgN_3 is rather slow (48 h at room temperature) due to a low solubility of AgN_3 in benzene, which can be accelerated by slightly increasing the temperature (24 h at 60 °C). However, with increasing temperature, diazide **2** tends to decompose slowly. This problem can be solved by using $Hg(N_3)_2$, which features a significantly better solubility, leading to full conversion within 30 min. Thermolysis reaction did not result in the formation of any isolatable product, e.g. nitridophosphorane, only unidentified brown decomposition products were spotted. Interestingly, photolysis led to regeneration of biradicaloid **1**Ter and the release of molecular nitrogen.

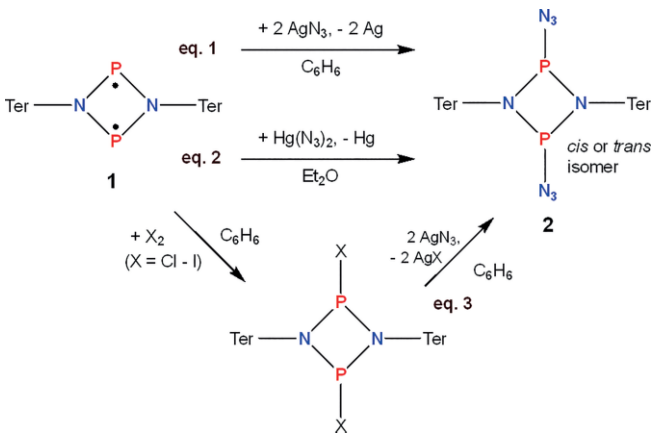

Scheme 4. Synthesis of $[N_3P(\mu\text{-NTer})]_2$ (**2**) starting either from $[P(\mu\text{-NTer})]_2$ or $[XP(\mu\text{-NTer})]_2$.

The novel synthesis concept featured in Scheme 4 (eq. 1 and eq. 2) can be generalized to a number of different X moieties: Utilization of AgX/HgX_2 (X = pseudohalogen, OR, SR etc.) leads first to oxidization of the phosphorus atom, which is accompanied by a transfer the X^- ion, affording the formation a P–X bond. For example, we also could demonstrate that treatment of $[P(\mu\text{-NTer})]_2$ with $Ag[CF_3CO_2]$ yielded $[CF_3C(O)OP(\mu\text{-NTer})]_2$ or with $Ag[BF_4]$ the fluorinated species $[F(\mu\text{-NTer})]_2$ and BF_3 besides Ag were isolated. Compared to the well-known X (X = Cl - I) / N_3 exchange, which also gives $[N_3P(\mu\text{-NTer})]_2$ (eq. 3) , our novel approach, starting from the biradicaloid $[P(\mu\text{-NTer})]_2$ (eq. 1 and eq. 2), has the advantage of generating halogen-free azide species. Often in case of classic X (X = Cl - I) / N_3 exchange reaction (Scheme 4, eq. 3), no complete exchange reaction is observed, which leads to a well-known X^- impurity problem, e.g. in

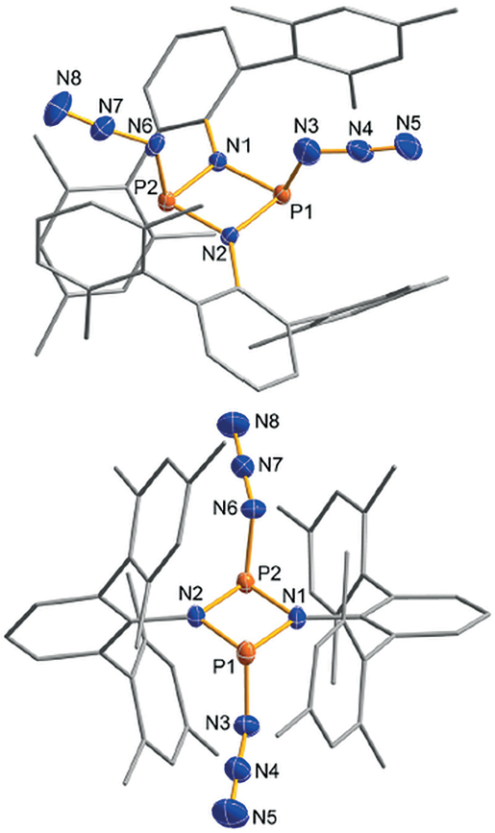

Figure 1. ORTEP representation of **2***cis* (top) and **2***trans* (bottom) in the crystal. Thermal ellipsoids correspond to 50% probability at 173 K. C atoms shown as wire-frame. Hydrogen atoms and disorder are omitted for clarity. Selected bond lengths (Å) and angles (°): **2***cis*: P1–N1 1.709(2), P1–N2 1.737(2); P1–N3 1.87(1), N3–N4 1.21(2), N4–N5 1.127(4), P2–N6 1.799(5), N6–N7 1.251(4), N7–N8 1.136(3), N5–N4–N3 169.1(7), N8–N7–N6 173.8(4), N4–N3–P1 110(1), N5–N4–N3 169.1(7); **2***trans*: P1–P2 2.6090(6), P1–N1 1.728(1), P1–N2 1.706(1), P1–N3 1.772(2), P2–N6 1.782(2), N3–N4 1.226(3), N4–N5 1.130(3), N6–N7 1.228(2), N7A–N8 1.130(3), N4–N3–P1 115.4(2), N5–N4–N3 174.3(3).

X-ray structure elucidations often a partial X occupation at the position of the azide group is observed.[59]

Diazido-*cyclo*-diphosphadiazane $[N_3P(\mu\text{-NTer})]_2$ was fully characterized and unequivocally characterized by single-crystal X-ray studies (Figure 1). As shown by ^{31}P NMR as well as X-ray studies, diazido species **2** exists as mixture of two isomers, **2***cis* and **2***trans*, respectively (Figure 1). Experimental solution ^{31}P NMR spectroscopic data in combination with computed NMR spectroscopic data reveal two isomers:[60] at 185.5 the *cis*-isomer and at δ = 242.3 ppm the *trans*- species in a ratio of 1(*cis*) : 0.25 (*trans*). According to gas phase DFT computation the difference between *cis* and trans diazido species is less than 1 kcal·mol^{-1}. The vibrational spectra (ATR-IR/Raman) of **2** confirmed the presence of azido groups as shown by the antisymmetric stretching mode $[\nu_{as}(N_3)]$ in the range 2100–2190 cm^{-1} and the symmetric stretching mode $[\nu_s(N_3)]$ at 1305–1241 cm^{-1}.[61] It is noteworthy to mention that due the existence of two azide groups per isomer two different ν_{as} / ν_s modes were observed corresponding to in-phase (2102 cm^{-1}, Raman active) and out-of-phase coupling (2092 cm^{-1}, IR active). X-ray structure elucidation revealed for both **2***cis* and **2***trans* *trans*-bent structure P–N_3 moiety well-known for covalently bound azides [Figure 1; N_α–N_β–N_γ angles, **2***cis*: 173.8(4) and **2***trans*: 174.3(3) Å].[61] The P–N_α bond lengths lie in the range 1.772(2) to 1.87(1) Å indicating single bonds [cf. Σr_{cov}(P–N) = 1.82 Å].[62] Interestingly, the P–N distances of **2***cis* are slightly longer than those of the *trans*-species [**2***cis*: 1.87(1) / 1.799(5) vs. **2***trans*: 1.772(2) / 1.782(2) Å]. Both diazides feature a planar P_2N_2 heterocycle (deviation from planarity <2°) with rather small P–N distances (between 1.70–1.74 Å) due to highly polarized bonds.

Addition of Covalent Azides

In a second series of experiments, we investigated the reaction of **1**Ter and **1**Hyp with different types of covalently bound organic azides yielding different types of Staudinger products. The following notations is used: All Staudinger-type products are denoted with the numeral **3**RR′**_I#**, where R is the substituent of the biradicaloid **1**R, R′ the substituent of the covalent azide, R′–N_3, and **I#** describes the formed isomer as depicted in Scheme 5.

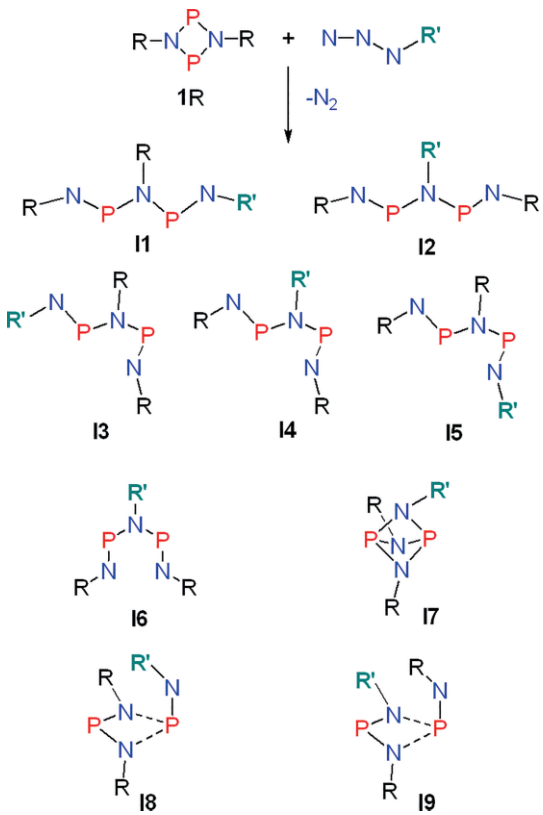

Scheme 5. Formal Staudinger products in the reaction of biradicaloid $[P(\mu\text{-NR})]_2$ (**1**R) with covalent azides R′-N_3 upon the release of molecular nitrogen, leading to the formation of different isomeric products (**3**RR'**_I#**), depending on the substituents (**I1** – **I9** computed isomers, see section on theory).

First, we treated **1**Ter with HN_3 and Me_3Si-N_3 in benzene. While in case of HN_3, a fast reaction was observed, leading to

many different species, which could not be isolated, we did not observe any reaction even at slightly elevated temperature (70 °C) for the reaction with Me_3Si-N_3. On the contrary, Mes-N_3 reacted readily with **1**Ter as could be seen by the evolution of molecular nitrogen. ^{31}P NMR experiments revealed only one singlet at δ = 296 ppm, which could be assigned to symmetric (*trans-trans*) triaza-diphospha-pentadiene, **3**TerMes_**I2** (Scheme 5, isomer **I2**), in accord with solid state X-ray structure analysis (Figure 2). No further products were observed. In contrast to a Staudinger reaction,[63–67] where a covalent azide reacts with a phosphine to give an iminophosphorane ($R_3P + R'N_3 \rightarrow R_3P{=}NR' + N_2$) along with the oxidation of the P^{III} to a P^V atom, the formation of a triaza-diphospha-pentadiene, R–N=P–N(R′)–P=N–R, indicates a new type of Staudinger reaction as no P^V-species is formed upon N_2 release and the formal two P(II) atoms in the biradicaloid are only oxidized to P^{III}. Moreover, beside the P–N bond making process, due to the Staudinger process, also P–N bond breaking and a structural rearrangement must have occurred (see theory section).

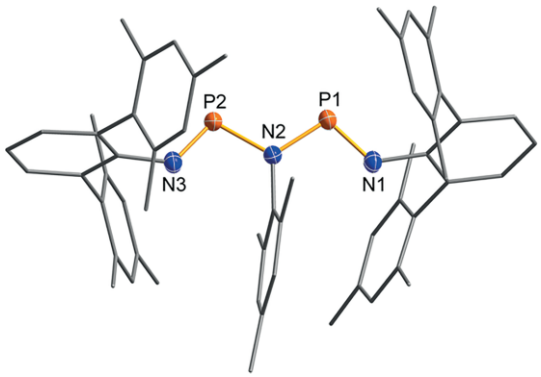

Figure 2. ORTEP representation of **3**Ter_Mes_**I2** in the crystal. Thermal ellipsoids correspond to 50 % probability at 173 K. C atoms shown as wire-frame. Hydrogen atoms omitted for clarity. Selected bond lengths (Å) and angles (°): P1–N1 1.541(1), P1–N2 1.697(1), P2–N3 1.538(1), P2–N2 1.702(1), N1–P1–N2 103.63(7), N3–P2–N2 103.80(7), N1–P2–N2-P2 175.9(8).

The first triaza-diphospha-pentadiene (an isomer of **3**TerMes_**I2**) was described by *Niecke* et al. even though they used a completely different approach. They treated chloro(arylimino)phosphanes with an 1,3-diaza-2-phosphaallylic species to give triaza-diphospha-pentadienes (Scheme 6).[68,69] This approach is limited to supermesityl-substituted species since Mes*–N=P–Cl is the only known monomeric iminochlorophosphane and the reaction yielded always isomer **3**Mes*R′_**I4** (Scheme 5 and Scheme 6) in the solid state.

As we knew from a theoretical study (vide infra), the reaction with covalent azide (model reaction **1**Ph with Me–N_3, see section on theory) can lead to many different structural, constitutional and conformational isomers, we used **1**Hyp instead of **1**Ter because **1**Hyp provides a smaller kinetic protection as can be seen from the smaller cone angle (Hyp: 213 vs. Ter: 232°).[70] Although the steric protection is much smaller as in **1**Ter, **1**Hyp still forms a biradicaloid without dimerization as long as non-polar solvents are used.[53] To explore the influ-

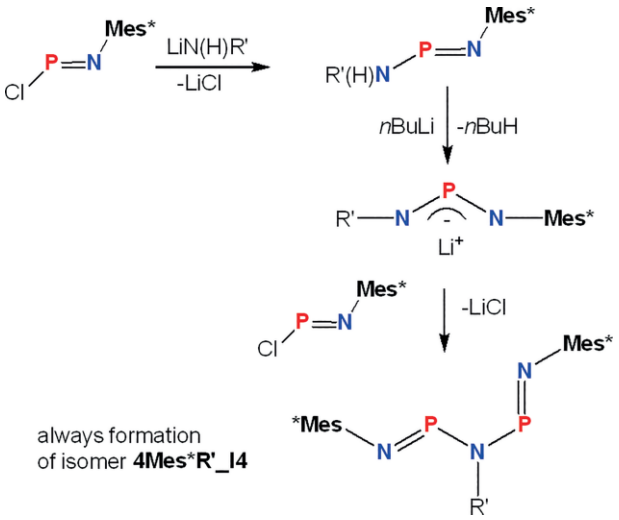

Scheme 6. Synthesis of supermesityl-substituted triaza-diphospha-pentadienes (isomer **4Mes*R'_I4**) according to *Niecke* et al. (R′ = *t*Bu, 2,4,6-*i*Pr$_3$C$_6$H$_2$, Mes*, trityl, adamantyl).[68,69]

ence of steric strain on the reaction, **1**Hyp was treated with covalent azides, R′–N_3, exhibiting a different steric strain [R′ = TMS = trimethylsilyl; Mes = mesityl, Dipp = (2,6-diisopropylphenyl), Mes* = supermesityl- = (2,4,6-tri-tert-butylphenyl), Table 1, Schemes 5–8].

Table 1. Products of the reaction of **1**Hyp with R-N_3 along with the maximal cone angle (mca, in °) and ^{31}P NMR shifts (ppm) of the product (Scheme 5 and Scheme 6) [a].

R′	Product	mca	^{31}Pa
TMS	**3_I2** [b]	142	350
Mes	[c]	220	[c]
Dipp	**3_I2**	223	301
Ter	**3_I5**	232	330br (308/354) [d,e]
Mes*	**4/4$_2$**	251	9.9(d), 382.5(dd) [f]

a) In [D$_6$]benzene, at 298 K. b) Besides **3** many other products, no isolation. c) Many products with resonances between 0–160 ppm, no isolation. d) 218 K – low-temperature data. e) Cf. ^{31}P MAS 307/356. f) $^2J(^{31}P\text{-}^{31}P)$ = 40, $^1J(^{31}P\text{-}^{14}N)$ = 22 Hz.

Generally, biradicaloid **1**Hyp was treated with R′–N_3 in *n*-hexane at ambient temperatures for ca. 5 min. However, in the case of the reaction with TMS-N_3 with **1**Hyp no conversion was observed even at slightly elevated temperatures and prolonged reactions times. After 5 h slow dimerization of **1**Hyp was detected rather than reaction with the azide. For this reason, we changed the synthesis protocol and carried out the reaction in a large excess of Me_3Si-N_3 without an additional solvent. Now an immediate reaction occurred leading to a whole bunch of different products as detected by ^{31}P NMR experiments. Amongst the ^{31}P NMR resonances we could assign the signal at δ = 350 ppm to triaza-diphospha-pentadiene **3**HypTMS_**I2** (Scheme 5, Table 1). Isolation of pure **3**HypTMS_**I2** failed (TMS = Me_3Si). A similar isolation problem was encountered in the reaction with Mes-N_3, which reacted within minutes yielding many different products (^{31}P NMR signals between 0 and 160 ppm).

To reduce the number of products (vide infra theoretical considerations), in the next series of experiments we utilized sterically encumbered azides to kinetically stabilize possible intermediates. Indeed, when using terphenyl azide, Ter-N_3, N_2 gas release was observed at once. Reduction of the solvent from the reaction mixture afforded red crystals, which were unequivocally proven to be triaza-diphospha-pentadiene **3**HypTer_**I5** (Figure 3 top, Table 1, Scheme 5). The existence of **3**HypTer_**I5** was also proven by ^{31}P NMR experiments in solution as well as in the solid state (^{31}P MAS). Interestingly, the ^{31}P NMR solution spectrum at ambient temperatures displayed only a broad singlet at δ = 330 ppm, which, however, split into two resonances at 218 K (354 and 308 ppm) as expected for two magnetically and chemically different P atoms in **3**HypTer_**I5** (Figure 3) in accord with computations and the ^{31}P MAS resonances (307/356 ppm). Obviously, at ambient temperatures a highly dynamic behavior due to a fast intramolecular isomerization process between species **3**HypTer_**I4**, **3**HypTer_**I5**, and **3**HypTer_**I3** (Scheme 5) is responsible for the singlet resonance (at 330 K).[68,69] Moreover, the formation of the "*trans-cis s-shaped*" conformation in **I5** indicates that the larger substituent (cone angles Hyp: 213 vs. Ter: 232°)[70] prefers the terminal position. Indeed, with slightly smaller substituents such as the diisopropylphenyl group, the reaction of Dipp-N_3 with **1**Hyp yielded the symmetric *trans-trans* product **3**HypDipp_**I2** (Table 1 and Scheme 5). **3**HypDipp_**I2** was isolated and fully characterized in solution (^{31}P NMR: 301 ppm) as well as solid state (Figure 3 bottom).

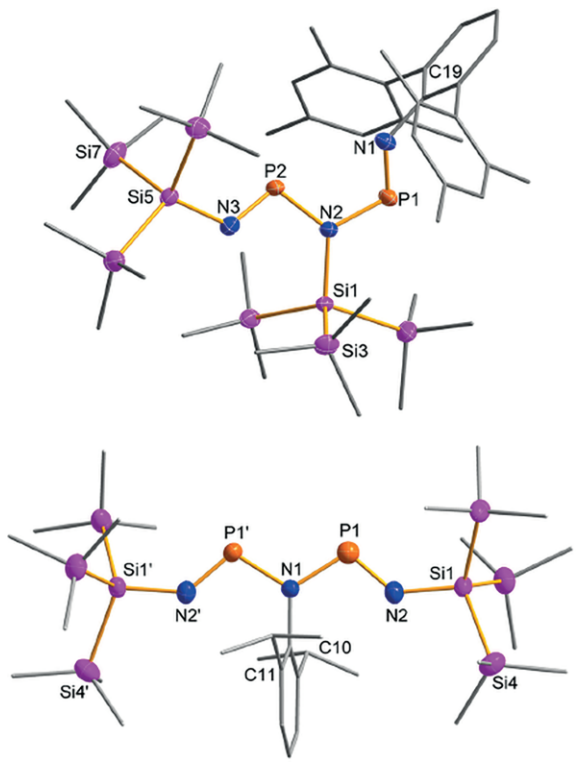

Figure 3. ORTEP representation of **3**HypTer_**I5** (top) and **3**HypDipp_**I2** (bottom) in the crystal. Thermal ellipsoids correspond to 50 % probability at 173 K. Carbon atoms shown as wire-frame. Hydrogen atoms are omitted for clarity. Selected bond lengths (Å) and angles (°) : **3**Hyp_Ter: P1–N1 1.553(2), P1–N2 1.676(2), P2–N2 1.717(2), P2–N3 1.549(3), N1–C19 1.411(3), N2–Si1 1.829(2), N3–Si5 1.777(3), Si1–Si3 2.353(2), Si5–Si7 2.359(2), N3–Si5–Si7 109.51(6),N1–P1–N2 105.02(9), N3–P2–N2 107.40(10), P1–N2–P2 116.1(1), C19–P1–N1 122.9(1), P2–N2–Si1 126.23(9), P2–N3–Si5 120.9(1), N1–P1–N2–P2 22.0(2), N3–P2–N2–P1 –165.8(1), N2–P1–N1–C19 –169.9(2), N1–P1–N2–Si1–161.8(1), N2–P2–N3–Si5 176.5(1). **3**Hyp_Dipp: P1–N1 1.710(2), P1–N2 1.531(2), N1–C10 1.449(2), N2–Si1 1.751(2), Si1–Si4 2.348(2), N2–P1–N1 107.16(7), C10–N1–P1 122.05(5), P1–N1–P1' 115.9(1), P1–N2–Si1 134.49(8), C11–C10–N1 118.8(1), N2–P1–N1–C10 0.72(6), N2–P1–N1–P1'–179.28(6), N1–P1–N2–Si1–173.25(9).

The azide with the largest steric hindrance (in this study) is the supermesityl azide, Mes*-N_3 (cone angle 251°). As depicted in Scheme 7, reaction of **1**Hyp with Mes*-N_3 resulted in a completely different reaction channel leading to the formation of a cyclo-diazaphosphetidine **4**HypMes*_**P6** (Figure 4 top, Scheme 8 corresponds to isomer **P6**) without release of molecular nitrogen.[71,72,81,82,73–80] The ^{31}P NMR spectrum featured two doublet resonances at 9.9 ppm for the four-coordinate and 382.5 ppm (^2J[^{31}P-^{31}P] = 39 Hz) for the two-coordinate phosphorus atoms. With a decomposition point of 91 °C, **4**HypMes*_**P6** is thermally less stable compared to the pentadienes (**3**HypDipp_**I2**: 122°, **3**HypTer_**I5**: 231 °C). While mounting dark-red crystals of **4**HypMes*′_**P6** under the microscope, another type (very small amount) of crystals was spotted.

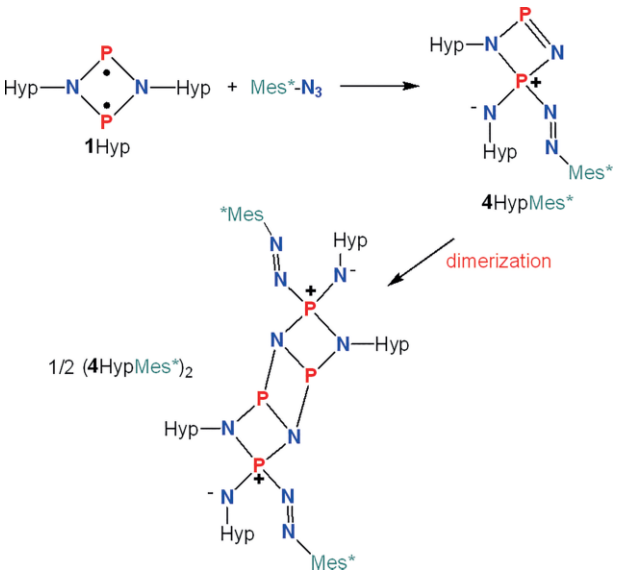

Scheme 7. Synthesis of **4**HypMes*_**P6** and (**4**HypMes*_**P6**)$_2$.

X-ray-structure elucidation revealed the presence of dimeric **4**HypMes*_**P6** (Figure 4 bottom). Obviously, dimerization to give (**4**Hyp_Mes*_**P6**)$_2$ occurs along the less protected P=N double bond at the two-coordinated P2 atom (Figure 4, Scheme 7). It was impossible to selectively run the reaction of **1**Hyp and Mes*-N_3 to give exclusively **4**HypMes*_**P6** as always oligomerization was observed. The formation of **4**HypMes*_**P6** is quite astonishing (Scheme 7 and Scheme 8) because it is neither the thermodynamically most preferred addition product nor is it more preferred than all compounds after the release of molecular nitrogen (Scheme 5). Hence, it can be

assumed that **4**HypMes*_**P6** is a kinetic favored product due to very bulky substituents.

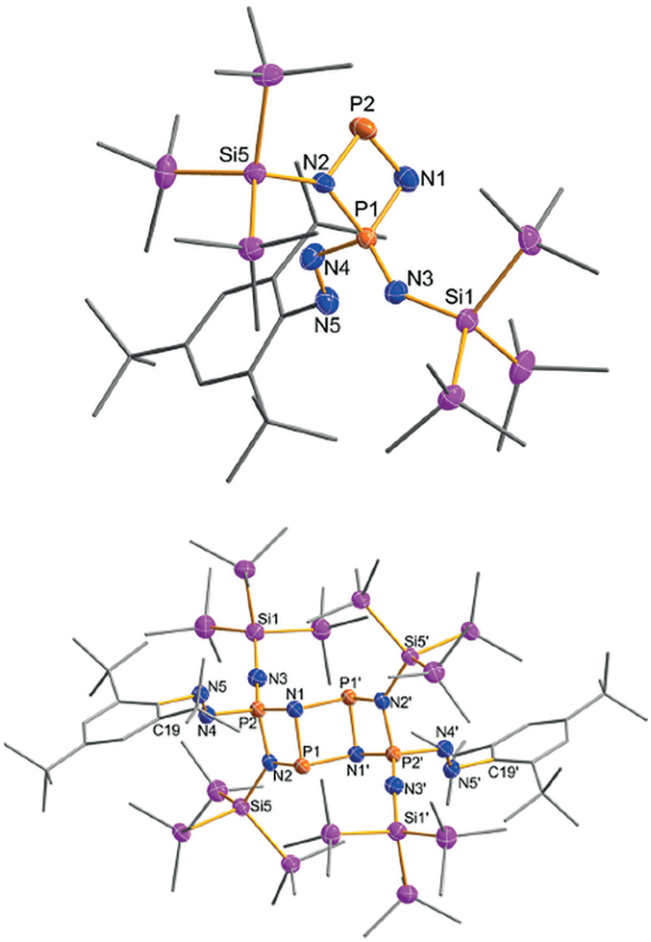

Figure 4. ORTEP representation of **4**HypMes*_**P6** (top, corresponds to isomer **P6** in Scheme 8) and its dimer (**4**HypMes*_**P6**)$_2$ (bottom) in the crystal. Thermal ellipsoids correspond to 50 % probability at 173 K. Carbon atoms shown as wire-frame. Hydrogen atoms are omitted for clarity. Selected bond lengths (Å) and angles (°): **monomer**: P1–N1 1.687(3), P1–N2 1.737(2), P1–N3 1.510(2), P1–N4 1.763(2), P1···P2 2.353(2), P2–N1 1.606(2), P2–N2 1.673(2), N4–N5 1.209(2), N5–C19 1.450(2), N3–Si11.735(2), N2–Si5 1.804(2), N3–P1–N2 121.06(7), N1–P1–N2 88.19(7), N3–P1–N4 116.37(8), N2–P1–N4 98.81(7), N1–P1–N2 43.03(5), N2–P1–P2 45.24(4), N1–P2–N2 93.21(7), P2–N1–P1 91.17(7), P2–N2–P1 87.27(6), N5–N4–P1 114.33(12), N1–P1–N2–P2 3.01(6), N4–P1–N2–P2 –98.61(7), N1–P1–N2–Si5 168.68(3), P2–P1–N3–Si1 –51.9(2), N1–P1–N4–N5 98.6(2), P1–N4–N5–C19 180.0(1); **dimer**: P2–N1 1.722(2), P2–N2 1.698(2), P2–N3 1.509(2), P2–N4 1.763(2), P1···P2 2.5479(8), P1–N1 1.783(2), P1–N2 1.742(2), N4–N5 1.254(2), N5–C19 1.459(3), N3–Si1 1.735(2), N2–Si5 1.819(2); N3–P2–N2 122.9(1), N1–P1–N2 83.52(8), N3–P2–N4 111.27(9), N2–P2–N4 98.88(8), N1–P2–N2 42.42(6), N2–P1–P2 41.54(6), N1–P2–N4 107.88(8), P2–N1–P1 93.24(8), P2–N2–P1 95.58(9), N5–N4–P2 117.1(1), N1–P2–N2–P1 –7.36(8), N4–P2–N2–P1 100.24(9), N1–P2–N2–Si5 –160.0(1), N3–P2–N1–P1 135.6(1), N2–P2–N1–P1 –7.16(8), P1–P2–N4–N5 –85.4(2), N5–C19–C20–C21–162.1(2).

Structure and Bonding of Triaza-diphospha-pentadienes, Diazaphosphetidine, and its Dimer

The structures of triaza-diphospha-pentadienes **3**TerMes_**I2**, **3**HypDipp_**I2**, **3**HypTer_**I5** and the azide adduct diazaphosphetidine, **4**HypMes*_**P6**, and its dimer (**4**HypMes*_**P6**)$_2$ were determined. Tables S1–S3 (Supporting Information) present the X-ray crystallographic data. Selected molecular parameters are listed below (see Figures 2–4).

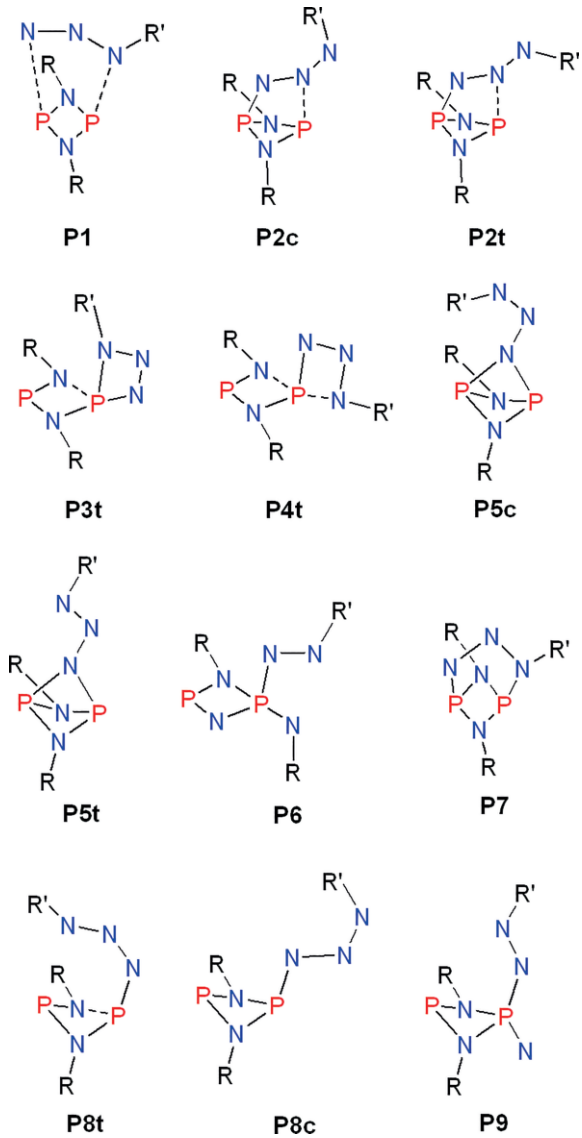

Scheme 8. Formal azide addition products of the reaction of biradicaloid [P(μ-NR)]$_2$ (**1**R) with covalent azides R'-N$_3$ (prior to the release of molecular nitrogen) leading to the formation of different isomeric products (**4**RR'_**I#**) depending on the substituents (**AI1** – **AI14**) computed isomers, see section on theory).

4HypMes*_**P6**, which can be realized as generated from an azide adduct species (see Scheme 8, Figure 4 top), crystallized in the monoclinic space group *C*2/*c* with eight formula units per cell, while its dimer, (**4**HypMes*_**P6**)$_2$ crystallized in the triclinic space group $P\bar{1}$ with $Z = 2$. In both species the hypersilyl-substituted P_2N_2 rings are slightly puckered (deviation from planarity 3.2° in the monomer, 7.1° in the dimer). However, the middle P_2N_2 ring of the ladder-type structural motif in the dimer is exactly planar (P1–N1–P1′–N1′ dihedral angle = 0.0°). In both compounds the P–N distances are in the range between 1.50–1.78 Å with the shortest distances always found

for the four-coordinated P^V atom attached to the N-Hyp moiety clearly indicating a double bond [cf. Σr_{cov}(P–N) = 1.82, Σr_{cov}(P=N) = 1.62 Å].[62] All other P–N bond lengths can be referred to polarized P–N single bonds. The N–N bond of the diazene units with 1.209(2) (monomer) and 1.254(2) Å (dimer) are in the expected range for N–N double bonds [Σr_{cov}(N=N) = 1.20 Å].[62] The three condensed four-membered P_2N_2 rings, forming a puckered ladder-type structure [N2–P1–N1′ 111.98(8)°], are an unusual motif in P–N chemistry. While the middle P_2N_2 ring is exclusively formed by P^{III} atoms, the left and right P_2N_2 rings are composed of alternating P^{III} and P^V atoms.

Two different types of Staudinger products, triaza-diphospha-pentadienes, could be isolated upon release of molecular nitrogen: While **3**TerMes_**I2** (monoclinic space group $P2_1/n$, Z = 4) and **3**HypDipp_**I2** (monoclinic space group $C2/c$, Z = 4) form a w-shaped N–P–N–P–N molecule, **3**HypTer_**I5** (monoclinic space group $P2_1/n$, Z = 4) exhibits a s-shaped triaza-diphospha-pentadiene unit. In both w-shaped species **3**, the NPNPN frame is essentially planar with local C_{2v} symmetry (deviation from planarity <5°) in agreement with the computed structure of the parent molecules HN=P–N(H)–P=NH. On the contrary, the NPNPN frame of the s-shaped species **3**HypTer_**I5** is strongly twisted with dihedral angles of 22.0(2) and 165.8(1)°. It can be assumed that the increased steric strain in **3**HypTer_**I5** is responsible to this large deviation from planarity as also the C_s-symmetric hydrogen substituted s-shaped parent molecule features a planar NPNPN frame. As expected for a heteroatomic 1,4-diyne and in agreement with the most favored Lewis representation, as depicted in Scheme 9, in all three species both terminal PN bonds are significantly shorter [1.541(1)–1.553(2), cf. Σr_{cov}(P=N) = 1.62 Å] compared to the two longer ones [1.676(2)–1.171(2), cf. Σr_{cov}(P–N) = 1.82 Å] along the central N–P–N.

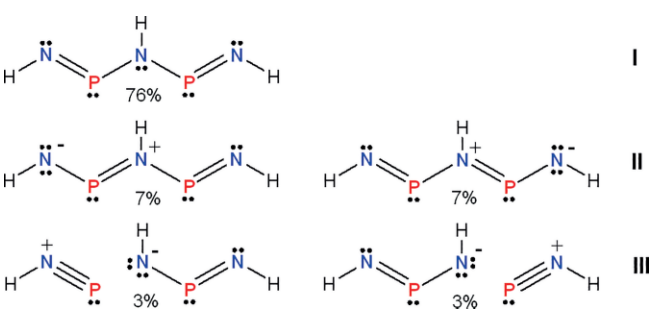

Scheme 9. Lewis representation from NRT (Natural resonance theory)[83,85,86] of triaza-diphospha-pentadiene **3**HH. Only those structures with a weight larger than 1 % are shown.

Note: the computed energy difference ($\Delta_{w-s}G°$) between the w- and the s-shaped parent molecules (**3**HH) is negligible (< 0.1 kcal·mol^{-1}), hence small differences in the steric repulsion between the substituents can favor either side. Both species are 6π-electronic systems with the best Lewis representation exhibiting two terminal P–N double bonds and one lone pair localized at the central N atom (Scheme 9, structure **I**). Delocalization of the lone pair is represented by Lewis structures of type **II** displaying conjugated double bonds and charge separation along one N–P–N unit. A small contribution stems from Lewis representation featuring a P–N triple bond (**III**). Both the P–N single as well as the double bonds are strongly polarized (ca. 70–80 % N / 30–20 % P) according to NBO (Natural bond analysis) analysis.[83,84] In agreement with the Lewis picture, there are three doubly occupied π-type molecular orbitals and the empty π* MO is the LUMO (Figure 5).

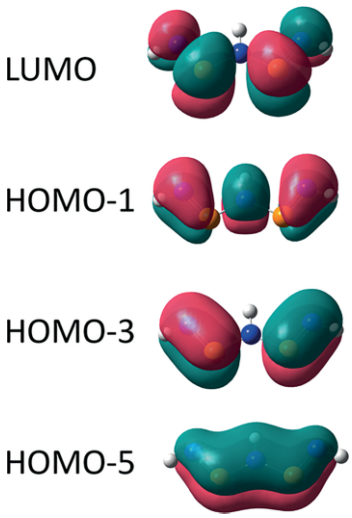

Figure 5. Molecular orbitals of the parent 6π-electronic triaza-diphospha-pentadiene w-**3**HH.

Theoretical Aspects – Thermodynamical and Kinetic Data of the Reaction of Biradicaloid 1 with Covalent Azides

To shed some light on the thermodynamics and mechanisms of the product formation as well as distribution in the reaction of biradicaloid **1** with covalently bound azides, quantum mechanical computations at the PBE/def2svp level of theory in conjunction with Grimme's dispersion correction[87,88] were performed.[89] Since the potential energy surface for the reaction of biradicaloid **1** with a covalent azide R-N_3 is rather complex, featuring many reaction channels as well as a plethora of different isomers (*cis-trans*, rotamers, etc.), we started with a model system (biradicaloid: [P(μ-N-Ph)]$_2$ (**1**Ph) and Me-N_3) to decrease the computational costs. First, a series of different potential energy surface scans were carried out considering six different approaches of either *trans*- or *cis*-azide, R–N_α–N_β–N_γ, to either one or both phosphorus atoms. To underline the complexity of this reaction, more than 30 isomers and more than 30 transition states (TS) could be localized on the (partly very flat) energy potential surface. Only the most important ones will be briefly discussed here. While the first three reactions pathways start with the approach of the N_β/N_γ atoms of *cis*-/*trans*-azide, respectively, to both P atoms [paths (i) and (ii)] and the N_γ of *cis*-azide to only one P atom, the other three ways begin with the attack of trans-azide via N_α/N_γ to one P atom [path (iv) and (v)] and only via N_α to one P atom [(vi) Scheme 10 and Scheme 11, Scheme 5 and Scheme 8]. The approaches (i) and (ii) may be considered [2+2] addition reactions. The transition states associated with

the first step of these six approaches are all in the range between 12.5 (TS2) – 27.5 (TS3) kcal·mol^{-1} (Table S8, Supporting Information), which means all these barriers can be overcome thermally at ambient temperatures. All other possible approaches were optimized to one of these six reaction channels.

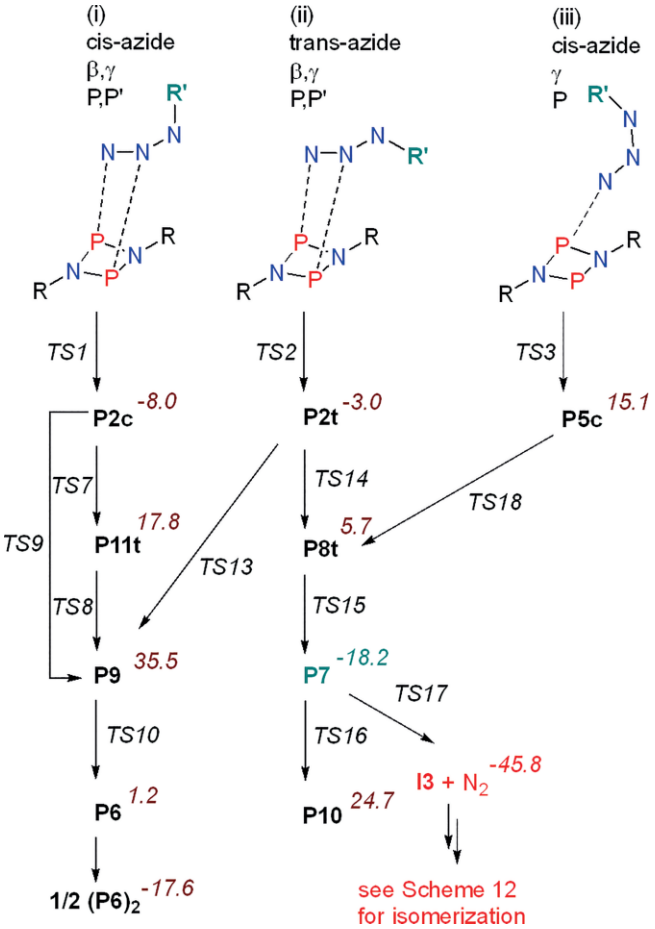

Scheme 10. Different reaction channels (I – iii) for the reaction of **1**Ph with Me-N_3 ($\Delta G°_{298}$ values (italics) relative to **1**Ph+MeN_3 in kcal·mol^{-1}, see Table 2, Tables S6–S10, Supporting Information).

The first reaction channel [path (i), Scheme 10 and Scheme 13] leads (for **1**Ph in the reaction with Me-N_3) only to thermodynamically unfavored, high-lying isomers besides **P2c** (Scheme 8), which is formed in an exergonic process. However, starting from **P2c** species **P9** is generated in a highly endergonic process, which seems to be necessary to for the formation of **P6** and its dimer that was observed for R = Hyp and R′ = Mes*. So far, we did find not any thermodynamically better path. The formation of the dimer (**P6**)$_2$ is exergonic for the overall process with –17.6 kcal·mol^{-1} but still much higher in energy than all products that release molecular nitrogen (**I1** – **I9**, Table 2 and Tables S6–S10, Supporting Information).

The second path leads in a straightforward exergonic reaction with small barriers (Tables S6–S10, Supporting Information) to the lowest-lying azide addition product **P7** ($\Delta_r G°_{298}$ = –18.2 kcal·mol^{-1}), a [3.1.1]bicyclic compound with a N_3 unit bridging the biradicaloid (Scheme 8 and Scheme 13), which decomposes upon eliminating N_2 to give triaza-di-

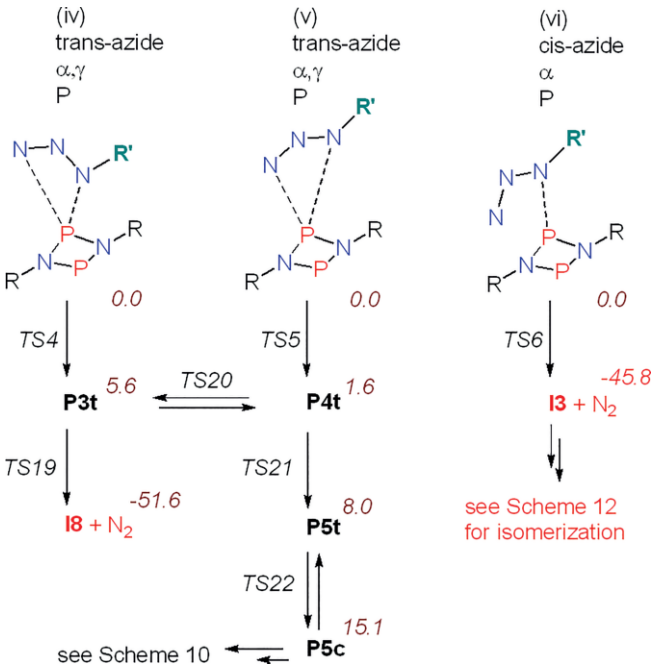

Scheme 11. Different reaction channels (iv – vi) for the reaction of **1**Ph with Me-N_3 ($\Delta G°_{298}$ values (italics) relative to **1**Ph+MeN_3 in kcal·mol^{-1}, see Table 1).

phospha-pentadienes **I3** in a highly exergonic process (–27.6 kcal·mol^{-1}) and an energy barrier to overcome of 10.7 kcal·mol^{-1}. Path iii provides [1.1.1]propellane **P5c**, which can easily be converted to **P8t**, which also passes through **P7**, as discribed for path (ii).

Reaction channels (iv) – (vi) are typical Staudinger type reactions with the formation of N_3P four-membered rings prior to the release of molecular nitrogen. However, since a second P atom is part of the conjugated NPNPN framework, the formal oxidation of one P^{III} atom to P^{V} is reduced by P–N bond cleavage, finally yielding triaza-diphospha-pentadienes **I1** – **I5** with the P atoms in the formal oxidation state +III. The isomers **I1** – **I5** can be easily converted into one another. As depicted in Scheme 12, there are two ways: Rotation around the P–N single bond (Scheme 9 Lewis structure **I**), e.g. **I3** → **I1** → **I5** (always with R′ in a terminal position) / **I2** → **I4** (always with R′ in the middle position, Scheme 5 and Scheme 12), or via ring opening in the [1.1.1]propellane. In the latter case, bond breaking in **I7** leads either to the formation of **I4** or **I5**, depending on which bond is cleaved. When isomer **I8** is formed, rotation around the R′N–P bond yields **I3**. The rotations are associated with barriers of ca. 10 kcal·mol^{-1} while barriers of ca. 20 kcal·mol^{-1} are found for the bond cleavage in **I7** (Tables S7–S10, Figure S6, Supporting Information). Therefore, these isomerization reactions should take place thermally (at ambient temperatures).

After understanding the reaction for the model system, we calculated the thermodynamic data for selected isomers using the experimentally used substituents R and R′. These data are summarized in Table 2. As can be seen from these data, all observed products are formed in exergonic processes. Espe-

Table 2. Gibbs free energies relative to **1**R + R′-N_3 (a) and relative to **2**RR′ (b) in kcal·mol^{-1} for isomers **I1** – **I5** and **P4t**.[a)]

R′	rel	I1	I2	I3	I4	I5	P4t
TMS	a	–38.2	–41.9	–43.6	–45.7	–42.3	11.9
	b	3.7	0.0	–1.7	**–3.8**	–0.3	53.8
Mes	a	–43.2	–53.3	–48.1	–51.4	–48.9	–7.1
	b	10.1	**0.0**	5.2	1.9	3.9	46.2
Dipp	a	–47.8	–57.3	–53.1	–55.6	–51.9	–8.3
	b	9.5	**0.0**	4.2	1.7	5.4	49.0
Ter	a	–43.3	–40.4	–49.2	–51.6	–55.9	–1.7
	b	–3.0	0.0	–8.8	–11.3	**–15.5**	38.7
Mes*	a	–36.5	–48.1	–40.9	–47.7	–52.0	–4.1
	b	11.5	0.0	7.2	0.3	**–3.9**	44.0

a) Values in bold represent the thermodynamically favored products.

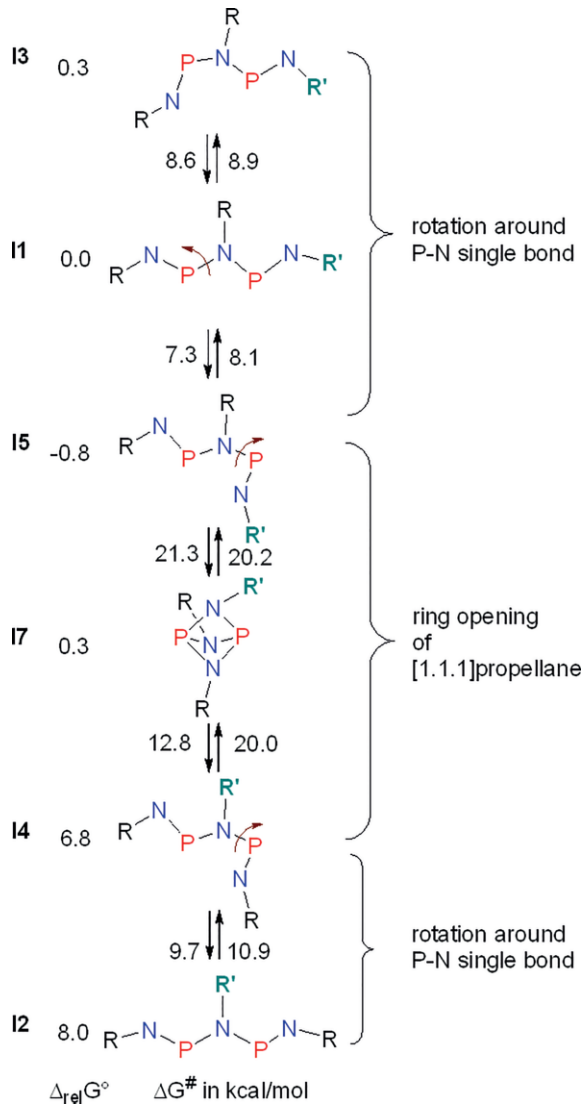

Scheme 12. Isomerization of compounds **I1** – **I7**.

cially, the release of molecular nitrogen is associated with a large energy gain. In accord with these data, experimentally observed isomer **I5** was found as most stable species for **3**HypTer and isomer **I2** for **3**HypDipp. Astonishingly, no isomer of **3**HypMes* was experimentally observed but the formation of **4**HypMes* as isomer **P4t**. Although formed in an exergonic process, the release of N_2 and the formation of **3**HypMes* as isomer **I5** should be thermodynamically much more favored by ca. 48 kcal·mol^{-1} (relative to **I5**) (Scheme 13). Obviously, **4**HypMes*_**P4t** is a kinetic product.

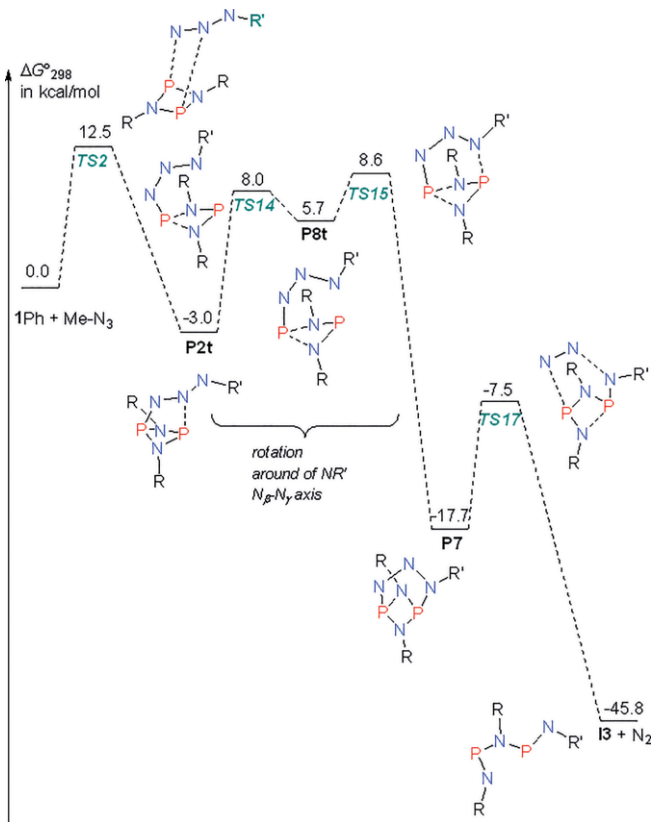

Scheme 13. Mechanism of the Staudinger-type reaction, **1**Ph + R′N_3, when two phosphorus atoms are involved.

Conclusions

Phosphorus centered biradicaloids **1**R, [P(μ-NR)]$_2$, were treated with ionic azides (AgN_3 and $Hg(N_3)_2$) leading in a redox-process to the formation of diazides, [N_3P(μ-NR)]$_2$ (R = Ter), and reduced metal, while triaza-diphospha-pentadienes could be isolated when covalent azides were added to **1**R (R = Ter, Hyp). On one occasion, we were able to isolate a high-lying isomer of an azide addition product (**4**HypMes*_**6**) and

its dimer. Theoretical studies of the azide addition reaction revealed a very soft potential energy surface with a huge number of different isomers. Finally, a short word with respect to the Staudinger type mechanism: As shown by Tian and Wang,[65] the classic Staudinger reaction exhibits two steps: (i) the *trans*-azide, $R'N_3$, attacks the P^{III} atom of a phosphane, R_3P, forming a chain-like *cis*-intermediate, R_3P-NNNR′ (*cis*-PNNN and *trans*-NNNR unit), and (ii) this intermediate forms a four-membered PN_3 ring, that dissociates easily into N_2 and $R_3P{=}NR'$, displaying a P^V atom. Due to the flat potential energy surface in the second step, the Staudinger reaction essentially requires one step to release N_2, which means that mostly no intermediate products can be isolated. In contrast, the potential energy surface for the reaction of biradicaloid **1**R with $R'N_3$ features different reactions channels including classic Staudinger type reactions with the formation of four-membered N_3P rings followed by the release of molecular nitrogen.

However, also a multi-step reaction [path (ii)] via a N_3-bridged cage-intermediate (**P7**, Scheme 13), which finally releases N_2 to give **I3**, is possible. Moreover, because a second P atom is present in the molecular frame, oxidation to a P^V species does not occur but the formation of a triaza-diphosphapentadienes featuring two P^{III} atoms. Since both P atoms can be described with the formal oxidation state +II in the biradicaloid, each P atom is oxidized by the loss of one electron. This also means a total loss of two electrons in accord with the oxidation of P^{III} to P^V in the typical Staudinger reaction when only one P^{III} atom is involved. Regarding the oxidation process and the mechanism, the reaction of the phosphorus-centered biradicaloid with a covalent azide represents a new variant of the Staudinger reaction.

Experimental Section

General Information: All manipulations were carried out under oxygen- and moisture-free conditions under argon using standard Schlenk or drybox techniques. Toluene was dried with Na/benzophenone, *n*-hexane was dried with Na/benzophenone/tetraglyme. All solvents were freshly distilled prior to use. Mes*-N_3, Ter-N_3 and Dipp-N_3 were prepared according to literature procedures.[90–92] Ph_3C-N_3 was prepared according to modified literature procedure.[93]

X-ray Structure Determination: X-ray quality crystals of all compounds were selected in Kel-F-oil (Riedel deHaen) or Fomblin YR-1800 perfluoroether (Alfa Aesar) at ambient temperatures. The samples were cooled to 173(2) K during measurement. The data were collected on a Bruker Apex Kappa-II CCD diffractometer using graphite-monochromated Mo-K_α radiation (λ = 0.71073). The structures were solved by direct methods[94] and refined by full-matrix least-squares procedures.[95] Semi-empirical absorption corrections were applied (SADABS).[96] All non-hydrogen atoms were refined anisotropically, hydrogen atoms were included in the refinement at calculated positions using a riding model.

Computational Details: Computations were carried out using Gaussian09[97] and the standalone version of NBO 6.0.[84,98–102] Structure optimizations were performed using the pure DFT functional PBE[103,104] in conjunction with Grimme's dispersion correction D3(BJ)[87,105] and the def2-SVP basis set[106] (notation PBE-D3/def2-SVP). All structures were fully optimized and confirmed as minima by frequency analyses. NRT analyses[85] of the DFT densities were computed to localize the electrons and obtain Lewis-type descriptions of the bonding patterns. It should be emphasized that all computations were carried out for single, isolated gas phase molecules. There may be significant differences between gas phase, solution and solid state.

Synthesis of 2: (*A*) $[P(\mu\text{-NTer})]_2$ (220 mg, 0.307 mmol) was dissolved in 5 mL toluene with stirring at room temperature. AgN_3 (94 mg, 0.627 mmol) was added to the orange solution in one portion. Immediately the solution turned dark, indicating the formation of elemental silver. Stirring overnight, however, did not lead to complete conversion. A further 121 mg (0.806 mmol) AgN_3 was added and stirred for another two days at room temperature. The resulting colorless suspension was filtered through diatomaceous earth and the colorless filtrate was concentrated until crystallization started and left to stand overnight, which led to the formation of colorless crystals. The mother liquor was removed by syringe and the crystals were dried under vacuum (124 mg, 0.155 mmol, 51 %). (*B*) $[IP(\mu\text{-NTer})]_2$ (239 mg, 0.246 mmol) was dissolved in 6 mL benzene with stirring at room temperature. AgN_3 (74 mg, 0.494 mmol) was added to the orange solution in one portion and stirred overnight at room temperature, resulting in a pale-yellow suspension. The solution was filtered through diatomaceous earth and the filtrate was concentrated until crystallization began. Colorless crystals were obtained after standing overnight untouched. The mother liquor was removed by syringe and the crystals were dried under vacuum (114 mg, 0.143 mmol, 58 %). (*C*) $[P(\mu\text{-NTer})]_2$ (151 mg, 0.211 mmol) and $Hg(N_3)_2$ (61 mg, 0.214 mmol) were weighed into a flask. To this end, 8 mL Et_2O was added and stirred for two hours at room temperature. In the meantime, the solution decolorized. Volatile components of the reaction mixture were removed under vacuum. The residue was added to 5 mL benzene and the solution filtered. The colorless filtrate was constricted in vacuo until crystallization began and left untouched for six hours, resulting in colorless crystals. The mother liquor was removed by syringe and the crystals dried in vacuo (130 mg, 0.162 mmol, 77 %). Mp.: 118 °C (dec.). EA found (calcd.): C 71.60 (71.98), H 6.37 (6.29), N 13.91 (13.99) %. **^{31}P NMR** (298 K, C_6D_6, 121.5 MHz): δ = 185.8 (s, *cis*), 242.3 (s, *trans*) ppm. **IR** (ATR): $\tilde{\nu}$ = 530 (m), 540 (m), 549 (m), 557 (w), 574 (m), 588 (w), 599 (m), 648 (m), 655 (m), 694 (m), 738 (m), 750 (m), 777 (m), 798 (m), 842 (s), 892 (s), 981 (s), 1031 (m), 1079 (s), 1091 (s), 1103 (s), 1124 (s), 1184 (s), 1224 (vs), 1305 (m), 1373 (w), 1378 (w), 1411 (m), 1440 (w), 1483 (w), 1567 (vw), 1581 (w), 1610 (w), 2092 (m), 2726 (vw), 2852 (w), 2914 (w), 2942 (w), 2998 (w) cm^{-1}. **Raman** (473 nm): $\tilde{\nu}$ = 223 (14), 245 (28), 272 (52), 339 (10), 370 (4), 406 (10), 451 (5), 494 (42), 512 (10), 528 (6), 549 (24), 567 (46), 579 (66), 595 (63), 657 (3), 740 (10), 903 (3), 913 (3), 945 (19), 972 (3), 1007 (7), 1033 (4), 1094 (40), 1161 (6), 1186 (5), 1247 (26), 1289 (100), 1304 (82), 1355 (4), 1379 (16), 1426 (88), 1481 (20), 1581 (90), 1611 (8), 2100 (5), 2724 (7), 2851 (22), 2912 (84), 3011 (17), 3042 (35), 3070 (19) cm^{-1}. **Raman** (632 nm): $\tilde{\nu}$ = 153 (34), 174 (11), 236 (22), 264 (12), 276 (18), 305 (13), 320 (10), 334 (12), 363 (12), 380 (17), 398 (19), 423 (28), 446 (4), 477 (7), 486 (13), 519 (32), 534 (9), 555 (17), 576 (100), 597 (15), 617 (4), 623 (4), 627 (4), 694 (10), 708 (13), 736 (15), 846 (6), 855 (6), 870 (5), 894 (4), 910 (4), 944 (16), 1006 (21), 1032 (6), 1040 (5), 1049 (5), 1098 (10), 1118 (5), 1130 (5), 1138 (5), 1159 (5), 1241 (18), 1285 (13), 1305 (82), 1341 (5), 1379 (30), 1404 (6), 1439 (14), 1481 (14), 1580 (18), 1609 (56), 2099 (8), 2727 (4), 2853 (11), 2918 (43), 2955 (14), 3009 (23), 3047 (14) cm^{-1}. **MS** (CI, pos., Isobutan) *m/z* (%): 330 (100) $[TerNH_3]^+$, 358 (11) $[TerNP]^+$, 386 (29) $[TerNH_2{+}C_4H_9]^+$, 687 (65) $[(TerNH)P]^+$, 716 (70) $[(TerNP)_2]^+$, 743 (9) $[M–4N–H]^+$, 801 (<1) $[M + H]^+$.

Synthesis of Triaza-diphospha-pentadiene (3TerMes_I2): To a stirred solution of TerNP (187 mg, 0.26 mmol) in benzene (3 mL), MesN3 was added (neat, 48 mg, 0.29 mmol). The initially orange solution did not undergo a significant change of color, but immediately evolution of gas was observable. The mixture was stirred for 30 min at room temperature and filtered afterwards (G4). The filtrate was concentrated until crystallization commences (ca. 0.5 mL) and left undisturbed overnight. The solution was removed via syringe and the solid was dried in vacuo at ambient temperature, yielding [TerNPN(Mes)PNTer] as an orange solid (91 mg, 0.11 mmol, 41 %). Mp: 182 °C (dec.). EA found (calcd.): C 79.26 (80.54), H 7.63 (7.23), N 4.80 (4.94) %. **^{1}H NMR** (298 K, C_6D_6, 250.1 MHz): δ = 1.16 [s, 6 H, *m*-CH_3(Mes)], 1.94 [s, 24 H, *o*-CH_3(Ter)], 2.13 [s, 3 H, *p*-CH_3(Mes)], 2.32 [s, 12 H, *p*-CH_3(Ter)], 6.61 [s, 2 H, *m*-CH(Mes)], 6.81 [br. s, 8 H, *m*-CH(Ter)], 6.89–6.98 (m, 6 H, m/p-CH). **^{31}P NMR** (298 K, C_6D_6, 121.5 MHz): δ = 296.0 (s) ppm. **IR** (ATR): $\tilde{\nu}$ = 3028 (w), 2999 (w), 2943 (w), 2914 (m), 2854 (w), 2729 (vw), 1610 (w), 1576 (w), 1558 (w), 1539 (vw), 1520 (vw), 1506 (vw), 1477 (m), 1458 (w), 1435 (m), 1416 (s), 1373 (m), 1342 (vw), 1308 (m), 1263 (vw), 1250 (w), 1221 (w), 1196 (m), 1182 (vw), 1157 (vw), 1144 (w), 1093 (w), 1078 (vw), 1031 (m), 1007 (m), 994 (w), 947 (vw), 893 (s), 860 (m), 849 (s), 798 (m), 785 (w), 764 (w), 752 (s), 741 (w), 714 (s), 679 (s), 650 (w), 617 (m), 602 (w), 598 (vw), 575 (vw), 563 (s) cm^{-1}. **Raman** (632 nm): $\tilde{\nu}$ = 3058 (11), 3040 (11), 30101 (14), 2915 (36), 2854 (11), 2729 (5), 1610 (27), 1579 (31), 1482 (15), 1435 (45), 1418 (100), 1381 (20), 1375 (19), 1357 (12), 1341 (18), 1313 (85), 1304 (90), 1284 (27), 1265 (15), 1250 (14), 1222 (10), 1195 (9), 1182 (12), 1164 (12), 1156 (12), 1143 (10), 1101 (15), 1092 (27), 1079 (11), 1039 (14), 1004 (15), 990 (20), 963 (9) 944 (11), 912 (15), 850 (5), 798 (4), 770 (7), 754 (11), 739 (8), 660 (4), 650 (10), 624 (12), 576 (43), 563 (15), 539 (17), 519 (17), 508 (7), 496 (6), 475 (4), 403 (7), 391 (12), 387 (12), 369 (8), 329 (11), 277 (4), 266 (5), 251 (7), 232 (30) cm^{-1}. **MS** (CI$^+$, isobutane) *m*/*z* (%): 164 (9) [MesNP]$^+$, 315 (5) [TerH+H]$^+$, 330 (18) [$TerNH_3$]$^+$, 358 (43) [TerNP]$^+$, 372 (3) [TerNPN]$^+$, 376 (5) [$TerNH_2$+C_4H_9]$^+$, 400 (4), 493 (80) [TerNPNMesH+H]$^+$, 535 (5), 549 (4) [TerNPNMesH+C_4H_9]$^+$, 671 (22), 687 (100) [TerNPNTerH+H]$^+$, 715 (12), 729 (5), 743 (10) [TerNPNTerH+C_4H_9]$^+$, 850 (22) [M + H]$^+$, 906 (3) [M+C_4H_9]$^+$. Crystals suitable for single-crystal X-ray diffraction experiments were obtained by cooling a saturated solution in diethyl ether to 4 °C overnight.

Synthesis of Triaza-diphospha-pentadiene (3HypTEr_I5): [P(μ-NHyp)]$_2$ (0.053 g, 0.09 mmol) and Ter–N_3 (0.033 g, 0.09 mmol) were solved in 5 mL *n*-hexane and stirred for 2 minutes at ambient temperature. The initial pink solution turned to deep red. The solvent was removed in vacuo yielding 0.028 g (0.031 mmol, 30 %) of [Hyp-NPN-(Hyp)PN-Ter] as a deep red microcrystalline solid. Mp.: 231 °C (dec.). EA found (calcd.): C 55.27 (55.12), N 4.60 (5.02), H 8.72 (8.63) %. **^{31}P{^{1}H} NMR** (25 °C, C_6D_6, 101.25 MHz): δ = 329.8 (s, 2P). **^{31}P MAS SSNMR** (25 °C, ss = 13 kHz): δ = 307 (s, 1P), 356 (s, 1P). **^{1}H NMR** (25 °C, C_6D_6, 250.13 MHz): δ = 0.25 [s, 54 H, (Si(Si(CH_3)$_3$)$_3$)$_2$], 2.21 (s, 12 H, *o*-CH_3), 2.26 (s, 6 H, *p*-CH_3), 6.88- 7.12 (m, 7 H, Ar-C*H*). **^{13}C{^{1}H} NMR** (25 °C, C_6D_6, 75.5 MHz): δ = 1.54 [s, (Si(Si(CH_3)$_3$)$_3$)$_2$], 21.25 (s, 4C, *o*-CH_3), 22.99 (s, *p*-CH_3), 128.86-136.35 (m, Ar-*C*H), 136.88- 153.55 (m, Ar-*C*). **^{29}Si{^{1}H} NMR** (25 °C, C_6D_6, 59.63 MHz): δ = –43.07- –42.09 [m, *Si*(Si(CH_3)$_3$)$_3$], –14.47- –13.27 [m, ^2J(^{29}Si-^{1}H) = 6.25 Hz, Si(*Si*(CH_3)$_3$)$_3$]. **^{29}Si CPMAS SSNMR** (25 °C, ss = 5 kHz): δ = –38.6- –43.8 [d, 2Si, *Si*(Si(CH_3)$_3$)$_3$], –11.8- –13.6 [d, 6Si, Si(*Si*(CH_3)$_3$)$_3$]. **IR** (ATR, 25 °C, 32 scans): $\tilde{\nu}$ = 2947 (w), 2893 (w), 1437 (w), 1408 (w), 1242 (m), 1136 (w), 1080 (w), 897 (m), 829 (vs), 798 (s), 770 (m), 752 (s), 735 (m), 687 (s), 663 (m), 621 (s), 600 (m) cm^{-1}. **Raman** (a: 70 mW, 25 °C, 50 scans): $\tilde{\nu}$ = 2950 (1), 2893 (3), 1161 (1), 1577 (1), 1436 (1), 1409 (5), 1304 (3), 1285 (4), 1135 (10), 1081 (2), 752 (1), 686 (1), 622 (3), 576 (2), 509 (1), 463 (1), 379 (2), 358 (1), 235 (1), 173 (4), 78 (6) cm^{-1}. **MS** (CI pos., *iso*-butane); *m*/*z* (%): 292 (10) [HypNP]$^+$, 307 (8) [HypNPN]$^+$, 330 (4) [Ter–NH_2]$^+$, 359 (3) [Ter–NP]$^+$ 555 (18) [HypNPNHyp]$^+$, 606 (1) [HypNPTer]$^+$, 620 (39) [HypNPNTer]$^+$, 912 (100) [M]$^+$, 913 (82) [M + H]$^+$. Crystals suitable for X-ray crystallographic analysis were obtained by a saturated *n*-hexane solution of [Hyp-NPN-(Hyp)PN-Ter] at ambient temperature.

Synthesis of Triaza-diphospha-pentadiene (3HypDipp_I2): To [P(μ-NHyp)]$_2$ (0.059 g, 0.10 mmol) was added 0.21 mL (0.10 mmol) of a solution of Dipp-N_3 in *n*-hexane (0.49 mol/L) and stirred for 2 minutes in 2 mL *n*-hexane at ambient temperature. The initial pink solution turned to orange. The solvent was removed in vacuo yielding 0.017 g (0.022 mmol, 22 %) of [Hyp-NPN-(Dipp)PN-Hyp] as a yellow microcrystalline solid. Mp.: 122 °C (dec.). EA found (calcd.): C 47.13 (46.62), N 5.50 (5.57), H 9.89 (8.96) %. **^{31}P{^{1}H} NMR** (25 °C, C_6D_6, 101.25 MHz): δ = 301.3 (s, 2P). **^{1}H NMR** (25 °C, C_6D_6, 250.13 MHz): δ = 0.23 [s, 54 H, (Si(Si(CH_3)$_3$)$_3$)$_2$], 1.24 [d, 12 H, ^3J(^{1}H-^{1}H) = 6.83 Hz, *o*-CH_3], 3.22 [sep., 2 H, ^3J(^{1}H-^{1}H) = 6.84 Hz, *o*-C*H*], 7.10- 7.14 (m, 3 H, Ar-C*H*). **^{13}C{^{1}H} NMR** (25 °C, C_6D_6, 75.5 MHz): δ = 0.01 [s, (Si(Si(CH_3)$_3$)$_3$)$_2$], 25.17 (s, *o*-CH_3), 29.98 (s, *o*-C*H*), 123.86 (s, 2C, *o*–Ar–C*H*), 132.85 (s, *m*–Ar–C*H*), 145.56 (s, 1C, *p*–Ar–C*H*). **^{29}Si{^{1}H} NMR** (25 °C, C_6D_6, 59.63 MHz): δ = –45.58- –44.47 [m, *Si*(Si(CH_3)$_3$)$_3$], –15.99- –14.35 [m, ^2J(^{29}Si-^{1}H) = 5.64 Hz, Si(*Si*(CH_3)$_3$)$_3$]. **IR** (ATR, 25 °C, 32 scans): $\tilde{\nu}$ = 2947 (w), 2891 (w), 1441 (w), 1394 (w), 1362 (vw), 1242 (s), 1207 (m), 1178 (m), 1101 (w), 1057 (vw), 1043 (vw), 926 (w), 827 (vs), 791 (s), 741 (m), 729 (m), 685 (s), 635 (m), 623 (m), 598 (s), 528 (s) cm^{-1}. **Raman** (a: 70 mW, 25 °C, 10 scans): $\tilde{\nu}$ = 3063 (1), 2949 (3), 2891 (5), 1589 (1), 1441 (1), 1405 (1), 1306 (1), 1248 (9), 1228 (9), 1179 (1), 1101 (1), 1041 (2), 928 (2), 887 (1), 867 (1), 836 (1), 728 (1), 690 (2), 654 (1), 621 (3), 612 (5), 542 (1), 467 (3), 393 (3), 356 (5), 267 (1), 220 (2), 206 (1), 164 (10), 133 (1), 110 (2) cm^{-1}. **MS** (CI pos., *iso*-butane); *m*/*z* (%): 178 (5) [Dipp–NH_3]$^+$ 292 (11) [HypNP]$^+$, 307 (2) [HypNPN]$^+$, 206 (1) [DippNP]$^+$, 453 (1) [HypNPDipp]$^+$, 467 (100) [HypNPNDipp]$^+$, 555 (1) [HypNPNHyp]$^+$, 584 (2) [[P(μ-NHyp)]$_2$]$^+$, 764 (7) [M]$^+$, 765 (2) [M + H]$^+$. Crystals suitable for X-ray crystallographic analysis were obtained by a saturated toluene solution of [Hyp-NPN-(Dipp)PN-Hyp] at –40 °C.

Synthesis of 1,3,2λ^3,4λ^4-Diazaphosphetidine (4HypMes*_P6): [P(μ-NHyp)]$_2$ (0.045 g, 0.08 mmol) and Mes*–N_3 (0.023 g, 0.08 mmol) were solved in 10 mL *n*-hexane and stirred for 5 minutes at ambient temperature. The resulting solution turned from orange to dark red. The solvent was removed in vacuo yielding 0.023 g (0.03 mmol, 35 %) of [Mes*NN-HypN(PN)$_2$Hyp] as a dark red/brown crystalline solid. Mp.: 98.1 °C (dec.). EA found (calcd.): C 49.55 (48.49), N 8.02 (7.06), H 9.59 (9.18) %. **^{31}P{^{1}H} NMR** (25 °C, C_6D_6, 101.25 MHz): δ = 9.9 [d, 1P, ^2J (^{31}P-^{31}P) = 40.37 Hz, *P*N$_2$], 382.5 [dd, 1P, ^2J (^{31}P-^{31}P) = 38.58, ^1J (^{31}P-^{14}N) = 21.70 Hz, *P*N$_5$]. **^{1}H NMR** (25 °C, C_6D_6, 250.13 MHz): δ = 0.17 [s, 27 H, Si(Si(CH_3)$_3$)$_3$], 0.47 [s, 27 H, Si(Si(CH_3)$_3$)$_3$], 1.29 (s, 9 H, *p*-CH_3), 1.50 (s, 18 H, *o*-CH_3), 7.46 (m, 2 H, Ar-*H*). **^{13}C{^{1}H} NMR** (25 °C, C_6D_6, 75.5 MHz): δ = 1.11 [s, Si(Si(CH_3)$_3$)$_3$], 1.19 [s, Si(Si(CH_3)$_3$)$_3$], 31.6 [s, *p*-C(CH_3)$_3$], 33.9 [s, *o*-C(CH_3)$_3$], 41.3 [s, *p*-*C*(CH$_3$)$_3$], 46.3 [s, *o*-*C*(CH$_3$)$_3$], 133.8- 147.4 (m, 6C, Ar-*C*). **^{29}Si{^{1}H} NMR** (25 °C, C_6D_6, 59.63 MHz): δ = –45.05 to –44.11 [m, *Si*(Si(CH_3)$_3$)$_3$], –16.58 to –13.06 [dm, ^3J (^{29}Si-^{31}P) = 65.35 Hz, Si(*Si*(CH_3)$_3$)$_3$]. **IR** (ATR, 25 °C, 32 scans): $\tilde{\nu}$ = 2951 (m), 2893 (w), 1594 (vw), 1477 (vw), 1464 (w), 1394 (w), 1362 (w), 1333 (s), 1242 (s), 1117 (w), 1007 (w), 974 (w), 827 (vs), 795 (s), 744 (s), 685 (s), 623 (s), 586 (m), 559 (m) cm^{-1}. **Raman** (a: 70 mW, 25 °C, 5 scans): $\tilde{\nu}$ = 3001 (3), 2952 (10), 2844 (2), 1727 (1), 1450 (1), 1178

(1), 1096 (3), 1087 (3), 991 (1), 987 (1), 969 (1), 811 (3), 600 (1), 574 (1), 568 (1), 561 (1), 557 (1), 367 (1) cm^{-1}. **MS** (CI pos., *iso*-butane); *m/z* (%): 245 (29) $[Mes^*]^+$, 247 (18) $[Hyp]^+$, 261 (8) $[Mes^*NH_2]^+$, 263 (10) $[HypNH_2]^+$, 275 (22) $[Mes^*N_2H_2]^+$, 292 (8) $[HypNP]^+$, 307 (59) $[HypNPN]^+$, 555 (18) $[HypNPNHyp]^+$, 876 (31) $[M]^+$, 877 (32) $[M + H]^+$. Crystals suitable for X-ray crystallographic analysis were obtained by a saturated *n*-hexane solution of [Mes*NN-HypN$(PN)_2$Hyp] at ambient temperature. Besides the crystals of **4**HypMes*_**P6**, crystals of a second kind were discovered and measured. This was the dimer (**4**HypMes*_**P6**)$_2$.

Supporting Information (see footnote on the first page of this article): ESI includes further details on the devices used, spectra, computational and X-ray data.

Acknowledgements

AS (Berlin, Glasgow, Munich) and AV (Munich) thank TMK for many great lectures and many inspiring discussions. Especially Berlin was a truly explosive time, in which AS learned everything about "*How to deal with azides*" as well as that sometimes it takes very long ways (e.g. to Budapest by car) and many borders must be overcome to be successful. Without this experience, this work would not have been possible. We are also indebted to the ITMZ of the University of Rostock for access to the high-performance computing facilities. Especially, we wish to thank *Malte Willert* for his continuous support with all software-related issues. We thank *Dr. Jonas Bresien* for helpful advice. Furthermore, we wish to thank the DFG (SCHU/1170/12–2) for financial support. Open access funding enabled and organized by Projekt DEAL.

Keywords: Azide; Phosphorus; Staudinger reaction; Biradicaloid; Reaction mechanisms

References

[1] J. P. Griess, *Philos. Trans. R. Soc. London* **1864**, *154*, 667–731.
[2] P. Griess, *Proc. R. Soc. London* **1864**, *13*, 375–384.
[3] T. Curtius, *Ber. Dtsch. Chem. Ges.* **1890**, *23*, 3023–3033.
[4] I. C. Tornieporth-Oetting, T. M. Klapötke, *Angew. Chem. Int. Ed. Engl.* **1995**, *34*, 511–520.
[5] M. Hargittai, I. C. Tornieporth-Oetting, T. M. Klapötke, M. Kolonits, I. Hargittai, *Angew. Chem. Int. Ed. Engl.* **1993**, *32*, 759–761.
[6] P. Buzek, T. M. Klapötke, P. von Ragué Schleyer, I. C. Tornieporth-Oetting, P. S. White, *Angew. Chem. Int. Ed. Engl.* **1993**, *32*, 275–277.
[7] T. M. Klapötke, A. Schulz, *Struct. Chem.* **1997**, *8*, 421–423.
[8] D. W. Stephan, G. Erker, *Angew. Chem. Int. Ed.* **2010**, *49*, 46–76.
[9] G. Erker, *Pure Appl. Chem.* **2012**, *84*, 2203–2217.
[10] D. W. Stephan, *J. Am. Chem. Soc.* **2015**, *137*, 10018–10032.
[11] D. W. Stephan, *Dalton Trans.* **2009**, *9226*, 3129–3136.
[12] G. Linti, H. Schnöckel, *Coord. Chem. Rev.* **2000**, *206–207*, 285–319.
[13] C. D. Martin, M. Soleilhavoup, G. Bertrand, *Chem. Sci.* **2013**, *4*, 3020–3030.
[14] M. Soleilhavoup, G. Bertrand, *Acc. Chem. Res.* **2015**, *48*, 256–266.
[15] M. Melaimi, M. Soleilhavoup, G. Bertrand, *Angew. Chem. Int. Ed.* **2010**, *49*, 8810–8849.
[16] D. Martin, M. Soleilhavoup, G. Bertrand, *Chem. Sci.* **2011**, *2*, 389–399.
[17] F. E. Hahn, M. C. Jahnke, *Angew. Chem.* **2008**, *120*, 3166–3216.
[18] U. Siemeling, C. Färber, C. Bruhn, M. Leibold, D. Selent, W. Baumann, M. von Hopffgarten, C. Goedecke, G. Frenking, *Chem. Sci.* **2010**, *1*, 697–704.
[19] D. Bourissou, O. Guerret, F. Gabbaï, G. Bertrand, *Chem. Rev.* **2000**, *100*, 39–92.
[20] O. Schuster, L. Yang, H. G. Raubenheimer, M. Albrecht, *Chem. Rev.* **2009**, *109*, 3445–3478.
[21] P. P. Power, *Chem. Rev.* **2003**, *103*, 789–810.
[22] G. He, O. Shynkaruk, M. W. Lui, E. Rivard, *Chem. Rev.* **2014**, *114*, 7815–7880.
[23] M. Abe, *Chem. Rev.* **2013**, *113*, 7011–7088.
[24] F. Breher, *Coord. Chem. Rev.* **2007**, *251*, 1007–1043.
[25] R. C. Fischer, P. P. Power, *Chem. Rev.* **2010**, *110*, 3877–923.
[26] P. P. Power, *Nature* **2010**, *463*, 171–177.
[27] E. Niecke, A. Fuchs, F. Baumeister, M. Nieger, W. W. W. Schoeller, *Angew. Chem.* **1995**, *107*, 640–642.
[28] O. Schmidt, A. Fuchs, D. Gudat, M. Nieger, W. Hoffbauer, E. Niecke, W. W. Schoeller, *Angew. Chem.* **1998**, *110*, 995–998.
[29] E. Niecke, A. Fuchs, M. Nieger, O. Schmidt, W. W. Schoeller, *Angew. Chem.* **1999**, *111*, 3216–3219.
[30] E. Niecke, A. Fuchs, M. Nieger, *Angew. Chem.* **1999**, *111*, 3213–3216.
[31] W. W. Schoeller, C. Begemann, E. Niecke, D. Gudat, *J. Phys. Chem. A* **2001**, *105*, 10731–10738.
[32] D. Scheschkewitz, H. Amii, H. Gornitzka, W. W. Schoeller, D. Bourissou, G. Bertrand, *Science* **2002**, *295*, 1880–1881.
[33] H. Grützmacher, F. Breher, *Angew. Chem.* **2002**, *114*, 4178–4184.
[34] M. Sebastian, M. Nieger, D. Szieberth, L. Nyulászi, E. Niecke, *Angew. Chem.* **2004**, *116*, 647–651.
[35] H. Sugiyama, S. Ito, M. Yoshifuji, *Angew. Chem.* **2003**, *115*, 3932–3934.
[36] C. Cui, M. Brynda, M. M. Olmstead, P. P. Power, *J. Am. Chem. Soc.* **2004**, *126*, 6510–6511.
[37] H. Amii, L. Vranicar, H. Gornitzka, D. Bourissou, G. Bertrand, *J. Am. Chem. Soc.* **2004**, *126*, 1344–1345.
[38] H. Cox, P. B. Hitchcock, M. F. Lappert, L. J.-M. Pierssens, *Angew. Chem.* **2004**, *116*, 4600–4604.
[39] P. Henke, T. Pankewitz, W. Klopper, F. Breher, H. Schnöckel, *Angew. Chem.* **2009**, *121*, 8285–8290.
[40] P. Henke, T. Pankewitz, W. Klopper, F. Breher, H. Schnöckel, *Angew. Chem. Int. Ed.* **2009**, *48*, 8141–8145.
[41] K. Takeuchi, M. Ichinohe, A. Sekiguchi, *J. Am. Chem. Soc.* **2011**, *133*, 12478–12481.
[42] S. H. Zhang, H. W. Xi, K. H. Lim, Q. Meng, M. B. Huang, C. W. So, *Chem. Eur. J.* **2012**, *18*, 4258–4263.
[43] Y. Hirano, G. Schnakenburg, R. Streubel, E. Niecke, S. Ito, *Helv. Chim. Acta* **2012**, *95*, 1723–1729.
[44] A. Hinz, A. Schulz, A. Villinger, *Chem. Commun.* **2016**, *52*, 6328–6331.
[45] A. Hinz, A. Schulz, A. Villinger, J.-M. Wolter, *J. Am. Chem. Soc.* **2015**, *137*, 3975–3980.
[46] E. Miliordos, K. Ruedenberg, S. S. Xantheas, *Angew. Chem.* **2013**, *125*, 5848–5851.
[47] J. Bresien, A. Hinz, A. Schulz, A. Villinger, *Dalton Trans.* **2018**, *47*, 4433–4436.
[48] A. Hinz, A. Schulz, A. Villinger, *Chem. Commun.* **2015**, *51*, 1363–1366.
[49] A. Hinz, A. Schulz, A. Villinger, *Angew. Chem. Int. Ed.* **2016**, *55*, 12214–12218.
[50] J. Bresien, A. Hinz, A. Schulz, A. Villinger, *Eur. J. Inorg. Chem.* **2018**, *2018*, 1679–1682.
[51] A. Hinz, R. Kuzora, U. Rosenthal, A. Schulz, A. A. Villinger, *Chem. Eur. J.* **2014**, *20*, 14659–14673.
[52] T. Beweries, R. Kuzora, U. Rosenthal, A. Schulz, A. Villinger, *Angew. Chem. Int. Ed.* **2011**, *50*, 8974–8978.
[53] A. Hinz, R. Kuzora, A. Rölke, A. Schulz, A. Villinger, R. Wustrack, *Eur. J. Inorg. Chem.* **2016**, *2016*, 3611–3619.

[54] S. Demeshko, C. Godemann, R. Kuzora, A. Schulz, A. Villinger, *Angew. Chem. Int. Ed.* **2013**, *52*, 2105–2108.
[55] A. Hinz, A. Schulz, *Phosphorus Sulfur Silicon Relat. Elem.* **2016**, *191*, 578–581.
[56] A. Hinz, A. Schulz, A. Villinger, *Angew. Chem.* **2015**, *127*, 2815–2819.
[57] A. Hinz, A. Schulz, A. Villinger, *Angew. Chem.* **2015**, *127*, 678–682.
[58] A. Hinz, A. Schulz, W. W. W. Seidel, A. Villinger, *Inorg. Chem.* **2014**, *53*, 11682–11690.
[59] K. Rosenstengel, A. Schulz, A. Villinger, *Inorg. Chem.* **2013**, *52*, 6110–6126.
[60] L. Stahl, *Coord. Chem. Rev.* **2000**, *210*, 203–250.
[61] I. C. Tornieporth-Oetting, T. M. Klapötke, *Angew. Chem.* **1995**, *107*, 559–568.
[62] P. Pyykkö, M. Atsumi, *Chem. Eur. J.* **2009**, *15*, 12770–12779.
[63] H. Staudinger, J. Meyer, *Helv. Chim. Acta* **1919**, *2*, 635–646.
[64] N. Götz, S. Herler, P. Mayer, A. Schulz, A. Villinger, J. J. Weigand, *Eur. J. Inorg. Chem.* **2006**, *2006*, 2051–2057.
[65] W. Q. Tian, Y. A. Wang, *J. Org. Chem.* **2004**, *69*, 4299–4308.
[66] J. E. Leffler, R. D. Temple, *J. Am. Chem. Soc.* **1967**, *89*, 5235–5246.
[67] H. Staudinger, E. Hauser, *Helv. Chim. Acta* **1921**, *4*, 861–886.
[68] E. Niecke, R. Detsch, M. Nieger, *Chem. Ber.* **1990**, *123*, 797–799.
[69] R. Detsch, E. Niecke, M. Nieger, F. Reichert, *Chem. Ber.* **1992**, *125*, 321–330.
[70] A. Schulz, *Z. Anorg. Allg. Chem.* **2014**, *640*, 2183–2192.
[71] H. J. Chen, R. C. Haltiwanger, T. G. Hill, M. L. Thompson, D. E. Coons, A. D. Norman, *Inorg. Chem.* **1985**, *24*, 4725–4730.
[72] E. J. Amigues, C. Hardacre, G. Keane, M. E. Migaud, *Green Chem.* **2008**, *10*, 660.
[73] G. David, E. Niecke, M. Nieger, V. Von Der Gönna, W. W. Schoeller, *Chem. Ber.* **1993**, *126*, 1513–1517.
[74] E. Niecke, D. Gudat, E. Symalla, *Angew. Chem.* **1986**, *98*, 817–818.
[75] C. Hering, M. Hertrich, A. Schulz, A. Villinger, *Inorg. Chem.* **2014**, *53*, 3880–3892.
[76] M. Lehmann, A. Schulz, A. Villinger, *Struct. Chem.* **2010**, *21*, 35–43.
[77] N. Burford, T. S. Cameron, K. D. Conroy, B. Ellis, M. Lumsden, C. L. B. Macdonald, R. McDonald, A. D. Phillips, P. J. Ragogna, R. W. Schurko, et al., *J. Am. Chem. Soc.* **2002**, *124*, 14012–14013.
[78] E. Niecke, D. Gudat, *Angew. Chem.* **1991**, *103*, 251–270.
[79] E. Niecke, D. Gudat, *Angew. Chem. Int. Ed. Engl.* **1991**, *30*, 217–237.
[80] R. Keat, L. Manojlovi-Muir, K. W. Muir, *Angew. Chem. Int. Ed. Engl.* **1973**, *12*, 311–312.
[81] O. J. Scherer, G. Schnabl, *Chem. Ber.* **1976**, *109*, 2996–3004.
[82] A. R. Davies, A. T. Dronsfield, R. N. Haszeldine, D. R. Taylor, *J. Chem. Soc. Perkin Trans. 1* **1973**, 379–385.
[83] E. D. Glendening, C. R. Landis, F. Weinhold, *J. Comput. Chem.* **2013**, *34*, 1429–1437.
[84] F. Weinhold, C. R. Landis, E. D. Glendening, *Int. Rev. Phys. Chem.* **2016**, *35*, 399–440.
[85] E. D. Glendening, F. Weinhold, *J. Comput. Chem.* **1998**, *19*, 593–609.
[86] E. D. Glendening, F. Weinhold, *J. Comput. Chem.* **1997**, *18*, 610–627.
[87] S. Grimme, S. Ehrlich, L. Goerigk, *J. Comput. Chem.* **2011**, *32*, 1456–1465.
[88] L. Goerigk, S. Grimme, *Phys. Chem. Chem. Phys.* **2011**, *13*, 6670.
[89] M. J. Frisch, G. W. Trucks, H. B. Schlegel, G. E. Scuseria, M. A. Robb, J. R. Cheeseman, G. Scalmani, V. Barone, B. Mennucci, G. A. Petersson, et al., **2009**.
[90] J. Das, S. N. Patil, R. Awasthi, C. P. Narasimhulu, S. Trehan, *Synthesis* **2005**, 1801–1806.
[91] K. Barral, A. D. Moorhouse, J. E. Moses, *Org. Lett.* **2007**, *9*, 1809–1811.
[92] F. Reiss, A. Schulz, A. Villinger, N. Weding, *Dalton Trans.* **2010**, *39*, 9962–9972.
[93] M. Kuprat, A. Schulz, A. Villinger, *Angew. Chem. Int. Ed.* **2013**, *52*, 7126–7130.
[94] G. M. Sheldrick, SHELXS-97 Progr. Solut. Cryst. Struct. Univ. Göttingen, Germany **1997**.
[95] G. M. Sheldrick, SHELXL-97 Progr. Refinement Cryst. Struct. Univ. Göttingen, Germany **1997**.
[96] G. M. Sheldrick, SADABS. Version 2. Univ. Göttingen, Germany **2000**.
[97] M. J. Frisch, G. W. Trucks, H. B. Schlegel, G. E. Scuseria, M. A. Robb, J. R. Cheeseman, G. Scalmani, V. Barone, B. Mennucci, G. A. Peterson, et al., **2013**.
[98] E. D. Glendening, J. K. Badenhoop, A. E. Reed, J. E. Carpenter, J. A. Bohmann, C. M. Morales, C. R. Landis, F. Weinhold, **2013**.
[99] J. E. Carpenter, F. Weinhold, *THEOCHEM* **1988**, *169*, 41–62.
[100] F. Weinhold, J. E. Carpenter, in *Struct. Small Mol. Ions* (Eds.: R. Naaman, Z. Vager), Springer, Boston, MA, **1988**, pp. 227–236.
[101] F. Weinhold, C. R. Landis, *Valency and Bonding. A Natural Bond Orbital Donor-Acceptor Perspective*, Cambridge University Press, **2005**.
[102] F. Weinhold, C. R. Landis, *Discovering Chemistry with Natural Bond Orbitals*, John Wiley & Sons, Inc., Hoboken, NJ, USA, **2012**.
[103] J. P. Perdew, K. Burke, M. Ernzerhof, *Phys. Rev. Lett.* **1996**, *77*, 3865–3868.
[104] J. P. Perdew, K. Burke, M. Ernzerhof, *Phys. Rev. Lett.* **1997**, *78*, 1396–1396.
[105] S. Grimme, J. Antony, S. Ehrlich, H. Krieg, *J. Chem. Phys.* **2010**, *132*, 154104.
[106] F. Weigend, R. Ahlrichs, *Phys. Chem. Chem. Phys.* **2005**, *7*, 3297.

Received: May 30, 2020
Published Online: November 3, 2020